

# Response Characteristics of Collapse Column in Coal Mining Working Face by Geoelectric Transillumination Method

Xingang Xu\*, Zhixin Liu, Jianhua Yue

School of Resources and Geosciences, China University of Mining & Technology, Xuzhou Jiangsu 221116, China  
 liuzhx@cumt.edu.cn

Geoelectric transillumination techniques are important tools for rich water structure investigations in coal mining work. To improve the application effect of this method, we researched the response characteristics of collapse column in coal mining working face based on FDTD numerical modelling with the singularity removal technique. We analysed impacts of some parameters such as spatial position, height, sectional area, resistivity of collapse column on electrical response of collapse column. The simulation result shows that the electrical response of "Through" type and "Concealed" type collapse column is inverted. The increasing of sectional area can enhance the exceptional response. The height of collapse column has a little impact on exceptional response for "Through" type collapse column. The curves of two injecting points of near collapse column can be used to locate flat position of collapse column. For "concealed" type collapse column, difference between the curves of two injecting points of near collapse column is unapparent, which can be used to judge the anomalous body is "through" type or "concealed" type. Exploration effect of geoelectric transillumination method apply to "Through" type collapse column is superior to "concealed" type.

## 1. Introduction

The collapse column is a special geological body, commonly encountered in coal mining, mainly distributed in carboniferous dyas coalfields in North China. The collapse column detection mainly adopts the drilling and geophysical prospecting methods. Surface geophysical prospecting methods can simply control large collapse column without sufficient accuracy. Mine radio wave penetration method and the slot wave method can detect the size and shape of collapse column in the working face very well, but it is difficult to get to know its water yield property, while geoelectric transillumination can determine the water yield property of collapse column. In-mine geoelectric transillumination method was introduced in 1986 (Csókás et al., 1986; Gyulai et al., 2013). In the former Soviet Union study this method in 1970~80's, and successfully detect the existence of collapse column in the suburb of Moscow. Han numerically simulated the 1D, 2D electrical response characteristics of the seven geoelectric transillumination arrays based on three-layered uniform layer geoelectric model (Han et al., 2000a; Han, 2000b; Liu et al., 2003; Shi, 2010). The result shows that seam sounding mainly reflects the electrical changes in the coal seam, the remaining six kinds arrays mainly reflects the electrical changes of the top and floor. Geoelectric transillumination method has been successfully applied in prevention and control of water detection on the working face, but its research on the electric response of the collapse column on the working face is not enough. This paper using three-dimensional finite difference method for simulation, mainly studies the electric response of some parameters such as spatial position, size, height, water transmissibility.

## 2. Methodology

### 2.1 The equation of stable current field and boundary conditions

The forward numerical simulation of geoelectric transillumination is to study the boundary value problem of the steady current field. For the active medium space, the stable current field satisfies the equation:

$$\nabla \cdot [\sigma(x, y, z) \nabla U] = -I \delta(x - x_0) \delta(y - y_0) \delta(z - z_0) \quad (1)$$

The  $\sigma(x, y, z)$  in the equation represents the conductivity of medium,  $U$  represents potential,  $(x_0, y_0, z_0)$  is the coordinate of the source and  $\delta$  is the Dirac function.

Equation (1) is a fundamental equations, definite condition are needed to gain definite solution. Direct current method is performing in the space of semi-infinite ground, but numerical methods can only solve field changes in limited space. To reduce the influence of the boundary truncation on the calculation results, the following boundary conditions are setted (Dey et al., 1979):

- (1)Ground boundary:  $\partial U/\partial n=0$ ;
- (2)Underground truncation boundary:  $\partial U/\partial n+U\cos\theta/r=0$ , where  $\theta$  is the included angle between radial vector  $\vec{r}$  from the source point to the boundary and the normal vector  $\vec{n}$ .

**2.2 Algorithm of singularity removal**

We use the integrated finite-difference approach to three-dimensional resistivity problem, introduced by Lowry (Lowry et al.,1989 )The calculation region is scattered to discrete systems made up of cuboid elements and nodes, the conductivity of the cuboid is  $\sigma_{i,j,k}$ , node potential is  $U_{i,j,k}$ .

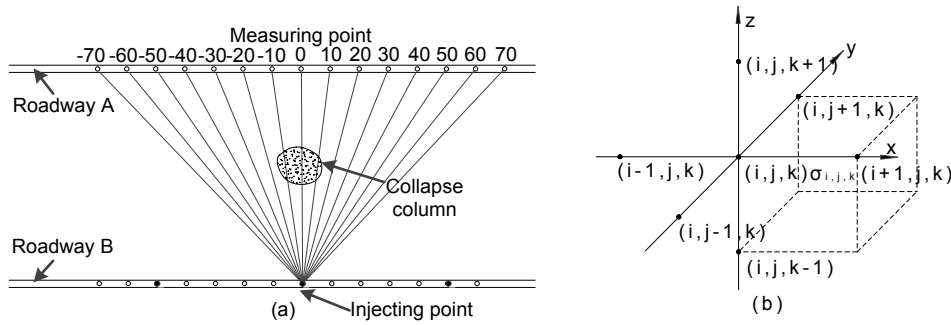


Figure1: (a) The set of injecting and measuring locations. (b) Mesh generation unit for FDTD method.

Since the potential function has singularity at the source point, in order to solve the calculation error caused by the singular point, the singular point removal algorithm is used. The potential function  $U$  is decomposed into normal field potentials  $U_s(x, y, z)$  and abnormal field potentials  $U_r(x, y, z)$ .

$$U(x, y, z) = U_s(x, y, z) + U_r(x, y, z) \tag{2}$$

where  $U_s(x, y, z)$  is potential generated by the current source in any point of the uniform medium, and  $U_r(x,y,z)$  represents potential generated by the anomalous body which is independence to the current source. Therefore, we have:

$$\nabla \cdot [\sigma \nabla (U_s + U_r)] = -I \delta(x - x_0) \delta(y - y_0) \delta(z - z_0) \tag{3}$$

The potential generated by the current source in a uniform medium whose electric conductivity is  $\sigma_m$  satisfies:

$$\nabla \cdot (\sigma_m \nabla U_s) = -I \delta(x - x_0) \delta(y - y_0) \delta(z - z_0) \tag{4}$$

Abnormal potential equation can be gained by using equation (3) minus equation (4):

$$\nabla \cdot [\sigma \nabla U_r] = -\nabla \cdot [(\sigma - \sigma_m) \nabla U_s] \tag{5}$$

where  $U_s$  can be calculated by formula  $U_s = I / (4\pi\sigma_m r)$ , where  $r$  is the distance to the current source. For computing numerical solution of equation (5), the derivative of the spatial distribution of conductivity is requested. Therefore, perform volume integral to both ends of equation (5), and using Green formula:

$$\iiint_{s_{i,j,k}} \sigma \frac{\partial U_r}{\partial n} ds_{i,j,k} = - \iiint_{s_{i,j,k}} (\sigma - \sigma_m) \frac{\partial U_s}{\partial n} ds_{i,j,k} \tag{6}$$

where  $s_{i,j,k}$  is the closed surface which surrounds the volume element  $\Delta v_{i,j,k}$ ,  $n$  is the outside normal direction of surface  $s_{i,j,k}$ . For rectangular mesh generation, grid node  $(i,j,k)$  is surrounded by a cuboid, e.g. Figure 1(b). Using difference instead of differential, equation (6) becomes:

$$\begin{aligned}
& C_{i,j,k}U_{i,j,k}^r + C_{i,j,k-1}U_{i,j,k-1}^r + C_{i,j,k+1}U_{i,j,k+1}^r + C_{i,j-1,k}U_{i,j-1,k}^r + C_{i,j+1,k}U_{i,j+1,k}^r + C_{i-1,j,k}U_{i-1,j,k}^r + C_{i+1,j,k}U_{i+1,j,k}^r \\
& = C'_{i,j,k}U_{i,j,k}^s + C'_{i,j,k-1}U_{i,j,k-1}^s + C'_{i,j,k+1}U_{i,j,k+1}^s + C'_{i,j-1,k}U_{i,j-1,k}^s + C'_{i,j+1,k}U_{i,j+1,k}^s + C'_{i-1,j,k}U_{i-1,j,k}^s + C'_{i+1,j,k}U_{i+1,j,k}^s
\end{aligned} \quad (7)$$

where coupling coefficient  $C$  and  $C'$  have the same calculation formula, the difference is only the electrical conductivity becoming  $\sigma_m - \sigma_{i,j,k}$  in  $C'$ , coupling coefficient  $C$  can be defined by the following formula:

$$C_{i-1,j,k} = \frac{1}{\Delta x_{j-1}} \left( \sigma_{i-1,j,k} \frac{\Delta y_j \Delta z_k}{4} + \sigma_{i-1,j,k-1} \frac{\Delta y_j \Delta z_{k-1}}{4} + \sigma_{i-1,j-1,k} \frac{\Delta y_{j-1} \Delta z_k}{4} + \sigma_{i-1,j-1,k-1} \frac{\Delta y_{j-1} \Delta z_{k-1}}{4} \right) \quad (7a)$$

$$C_{i+1,j,k} = \frac{1}{\Delta x_j} \left( \sigma_{i,j,k} \frac{\Delta y_j \Delta z_k}{4} + \sigma_{i,j,k-1} \frac{\Delta y_j \Delta z_{k-1}}{4} + \sigma_{i,j-1,k} \frac{\Delta y_{j-1} \Delta z_k}{4} + \sigma_{i,j-1,k-1} \frac{\Delta y_{j-1} \Delta z_{k-1}}{4} \right) \quad (7b)$$

$$C_{i,j-1,k} = \frac{1}{\Delta y_{j-1}} \left( \sigma_{i-1,j-1,k} \frac{\Delta x_{j-1} \Delta z_k}{4} + \sigma_{i,j-1,k} \frac{\Delta x_j \Delta z_k}{4} + \sigma_{i-1,j-1,k-1} \frac{\Delta x_{j-1} \Delta z_{k-1}}{4} + \sigma_{i,j-1,k-1} \frac{\Delta x_j \Delta z_{k-1}}{4} \right) \quad (7c)$$

$$C_{i,j+1,k} = \frac{1}{\Delta y_k} \left( \sigma_{i-1,j,k} \frac{\Delta x_{j-1} \Delta z_k}{4} + \sigma_{i-1,j,k-1} \frac{\Delta x_{j-1} \Delta z_{k-1}}{4} + \sigma_{i,j,k} \frac{\Delta x_j \Delta z_k}{4} + \sigma_{i,j,k-1} \frac{\Delta x_j \Delta z_{k-1}}{4} \right) \quad (7d)$$

$$C_{i,j,k-1} = \frac{1}{\Delta z_{j-1}} \left( \sigma_{i,j,k-1} \frac{\Delta x_i \Delta y_j}{4} + \sigma_{i,j-1,k-1} \frac{\Delta x_i \Delta y_{j-1}}{4} + \sigma_{i-1,j,k-1} \frac{\Delta x_{j-1} \Delta y_j}{4} + \sigma_{i-1,j-1,k-1} \frac{\Delta x_{j-1} \Delta y_{j-1}}{4} \right) \quad (7e)$$

$$C_{i,j,k+1} = \frac{1}{\Delta z_j} \left( \sigma_{i,j,k} \frac{\Delta x_i \Delta y_j}{4} + \sigma_{i,j-1,k} \frac{\Delta x_i \Delta y_{j-1}}{4} + \sigma_{i-1,j,k} \frac{\Delta x_{j-1} \Delta y_j}{4} + \sigma_{i-1,j-1,k} \frac{\Delta x_{j-1} \Delta y_{j-1}}{4} \right) \quad (7f)$$

$$C_{i,j,k} = -(C_{i+1,j,k} + C_{i-1,j,k} + C_{i,j+1,k} + C_{i,j-1,k} + C_{i,j,k+1} + C_{i,j,k-1}) \quad (7g)$$

For the potential solving of all nodes in a limited area, it becomes a problem of solving larger linear system of equations. Through the method above, the boundary value problem of steady current fields transformed to a linear system of equations to solve abnormal potential of each discrete node, the incomplete Cholesky decomposition conjugate gradient method (ICCG method) is used to solve this large, sparse equation sets.

### 3. Collapse column 's electrical response characteristics

#### 3.1 "Through" type collapse column

For the research of response characteristics of collapse column by geoelectric transillumination, three layers geoelectric model with collapse column has been designed. The model comprises a collapse column throughout the coal seam, e.g. Figure 2(a). Coal-seam thickness  $d$  is equal to 8 meters. The cross section length of the anomalous body is  $l$ , and the height is  $h_1 + d + h_2$ . The resistivity parameters are as following : roof,  $\rho = 60 \Omega m$ ; floor,  $\rho = 80 \Omega m$ ; coal,  $\rho = 500 \Omega m$ . The spatial relationship of anomalous body and coal mining working face is shown in Figure 2(b). The inclined length of coal mining working face is 150 meters. The interval of injecting points is 50 meters, and the interval of measuring points is 10 meters.

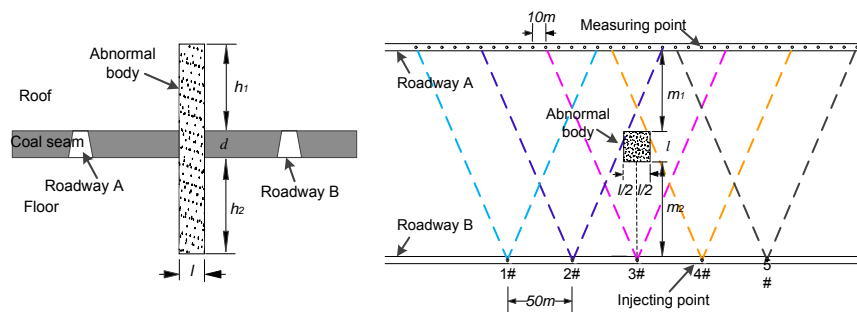


Figure 2: (a) Cross-section (b) Plan. The measuring scope is denoted by different colours dotted lines

According to water yield property, collapse column can be divided into rich-water and water resistant. They usually show as low-resistivity and high-resistivity. Their resistivities are respectively given  $5 \Omega m$  and  $2000 \Omega m$ . The height of anomalous body is 200 meters. Other parameters are  $l = 30$  meters,  $m_1 = 60$  meters,  $m_2 = 60$

meters, respectively. Electrical characteristics of low-resistivity and high-resistivity collapse column are shown in Figure 3. The potential curves are separately corresponding to No.1,2,3,4,5 injecting point and normal model. The position relationship between measuring point and injecting is described in Figure 1(a). In this paper, normal model refers in particular to a three-layered model without any anomalous body whose parameters are as before. Curve of normal model is called "normal curve".

From Figure 3(a), it is obviously that the normal potential curve (denoted by red cross) is symmetry about the line  $x=0$ . The distance from potential value to injecting point is inversely proportional to the distance of measuring point. When high-resistivity collapse column is on the path of injecting point to acceptance point, the move of the charge will encounter greater resistance. Therefore, current density  $J$  inside and nearby the high-resistivity collapse column will be decreased. As a result, if the path is closed to the anomalous body, measuring potential value is less than value of normal model on the same measuring point. This can be verified by the comparison between 3# curve and normal curve. By analyzing 2# and 4# curve, it can be found that measuring potential value become smaller when the path is moving closer to the anomalous body. According to these characteristics, horizontal position of abnormal body can be located by determining separation point on 2# and 4# curve. Furthermore, we can see that 1# ,5# curve and normal curve almost overlap, which indicates that the impact on current transmission is gradually weakened along with the path moves away from the anomalous body.

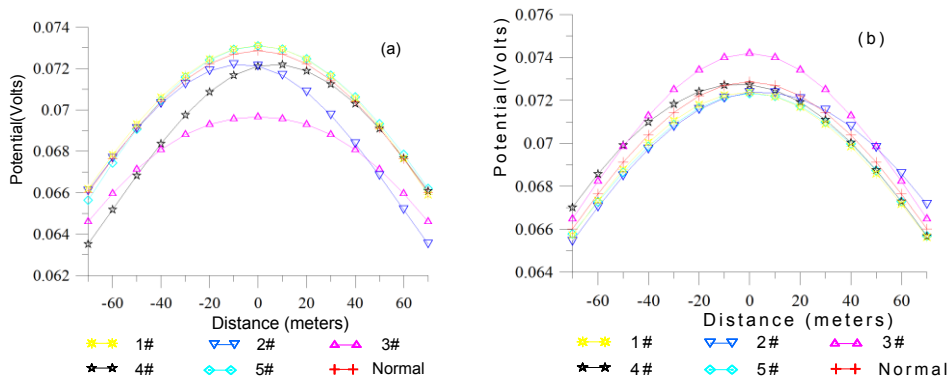


Figure 3: (a) The high-resistivity collapse column

(b) The low-resistivity collapse column

For low-resistivity collapse column model, moving of the charge near anomalous body encounters lesser resistance. This can lead to measuring potential value large than the normal model (compare 3# curve to normal curve in Figure 3(b)). Locating abnormal body and the influence rule of distance on current transmission is like above.

The low-resistivity collapse column had a greater influence on coal mine water inrush than high-resistivity one, so only low-resistivity collapse column is discussed. That is, the resistivity of abnormal body is  $5 \Omega\text{m}$  in the following passage. The measuring potential values are controlled by space form change, such as cross-sectional area, height of abnormal body and distance from abnormal body to roadway. These will be discussed below.

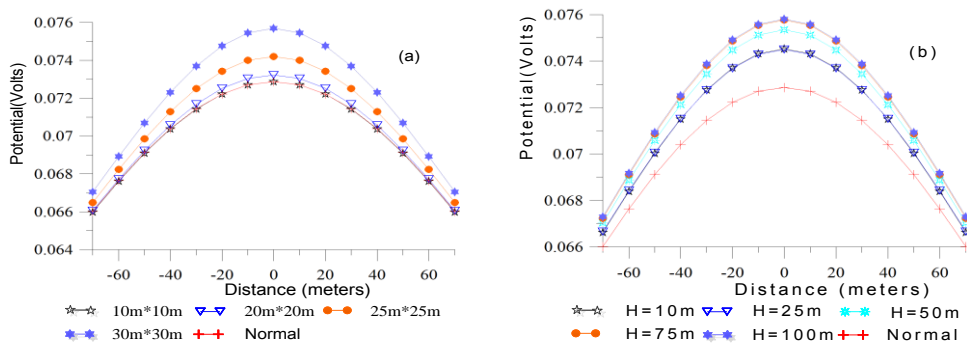


Figure 4: (a) Impacts of sectional area change

(b) Impacts of height change.

Figure 4(a) shows impact on potential response which is due to cross-sectional area change of anomalous body. These curves are corresponding to 3# injecting point. Here, the height of anomalous body is 200 meters. Other parameters except  $l$ ,  $m_1$ ,  $m_2$ , are same as above. From the figure, it is obviously that potential values are increased with the increasing of edge length  $l$ . When  $l$  is equal to 10 meters, curve and normal curve almost overlap, so the anomalous body is difficult to distinguish.

Influence of the height change on measuring potential value is shown in Figure 4(b). These curves are also corresponding to 3# injecting point. The edge length  $l$  is equal to 30 meters, and  $m_1$  or  $m_2$  is equal to 60 meters. Other parameters except the height of anomalous body are same as above. Compare curves with  $H=10, 25, 50, 75, 100$  meters to normal curve, we can see that potential values of "through" type collapse column model with different heights are obviously greater than the one of normal model, which indicates that the height of collapse column has little impact on measuring values. Measuring values has a little change when  $H<25$  meters or  $H>75$  meters. This result is possibly related to the distribution of the current line.

Measuring value is changed with vary of the distance  $m_2$  (as shown in Figure 5). The edge length  $l$  is equal to 30 meters, and the height of anomalous body is 200 meters. Other parameters except the distance  $m_2$  are same as above. When anomalous body is closer to injecting point, measuring values ( $m_2=40$  meters) is observably increased. The reason is that more current is absorbed in anomalous body. Moreover, measuring values of both sides are rapidly decreased with the increasing of  $m_2$ , because of the path between injecting point and measuring point in two sides is gradually moving away from anomalous body.

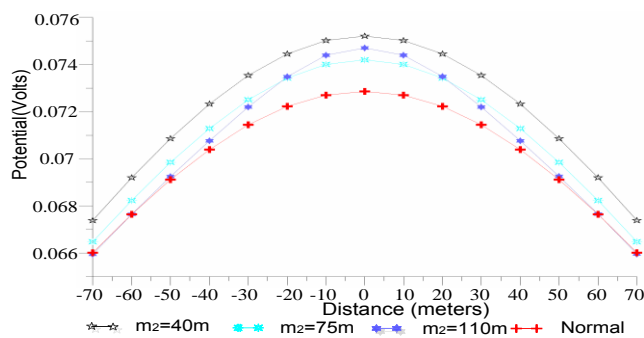


Figure 5: Variation of potential response with the changing of distance  $m_2$ .

### 3.2 Response characteristics of concealed collapse column under the coal seam

The concealed collapse column model is shown in Figure 6. The model comprises an anomalous body with a resistivity of  $\rho=5 \Omega \text{ m}$  under the coal seam. Height of the anomalous body is  $h_2=200$  meters, and the distance from coal seam to the top of collapse column is  $h_1$ . The location relationship between anomalous body and coal mining working face is shown in Figure 2 (b). The parameters are as following:  $l=30$  meters,  $m_1=m_2=60$  meters; roof,  $\rho=60 \Omega \text{ m}$ ; floor,  $\rho=80 \Omega \text{ m}$ ; coal,  $\rho=500 \Omega \text{ m}$ .

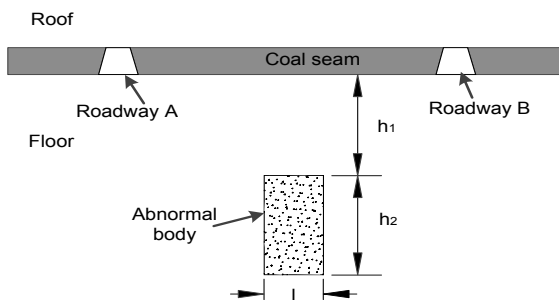


Figure 6: Concealed collapse column model.

Measuring potential value less than the value of normal model is a major response characteristic of concealed low-resistivity collapse column (as shown in Figure 7(a)). This is different from "through" type collapse column model. The main reason of the above results is current density decreasing on the path from injecting point to measuring point which caused by the attraction to current of low-resistivity body under the coal seam. Difference between 2# and 4# curve is unapparent, so it is difficult to locate the anomalous body by analysing

2#, 4# curve. Nevertheless, this conclusion can be used to judge the anomalous body is "through" type or "concealed" type. From Figure 7(b), we can see that measuring potential values are gradually increased with the increasing of  $h_1$ . After  $h_1$  is greater than 150 meters, potential curve of anomalous model is almost overlap with the normal curve.

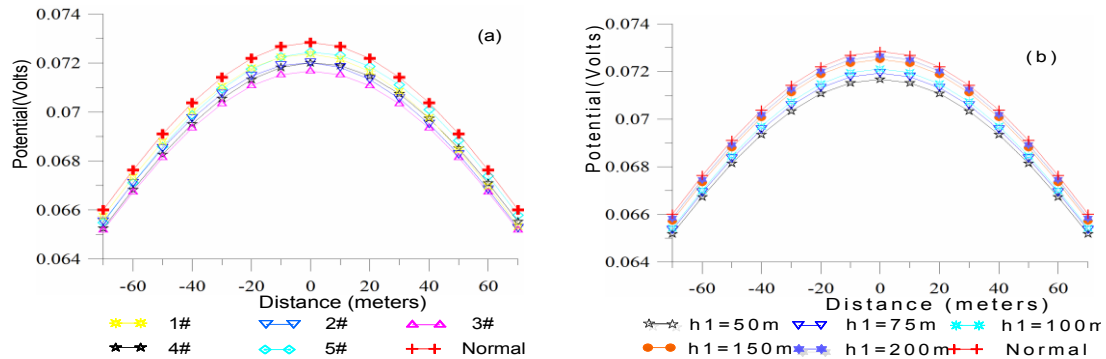


Figure 7:(a) potential responses corresponding to 1~ 5 # injecting point with  $h_1=50$  meters, (b) Potential responses corresponding to 3# injecting point with  $h_1=50, 75, 100, 150, 200$  meters.

#### 4. Conclusion

In this paper, we have proposed a 3-D finite-difference scheme for DC resistivity modeling based on the singularity removal technique. We have researched the electrical response characteristics of collapse column with three-layers geoelectric model by this numerical algorithm. For "Through" type collapse column, the height of collapse column has a little impact on measuring values. The increasing of sectional area can enhance the response. Electric character of collapse column close to the injecting point is observably different from one near measuring point. The curves corresponding to injecting points adjacent to the two sides of collapse column can be used to locate horizontal position of collapse column. For "concealed" type collapse column, difference among the curves corresponding to injecting points adjacent to the two sides of collapse column is unapparent. This conclusion can be used to judge anomalous body is "through" type or "concealed" type.

#### Reference

- Csókás J., Dobróka M., Gyulai Á., 1986, Geoelectric determination of quality changes and tectonic disturbances in coal deposits, *Geophysical Prospect*, 34, 1067-1081, DOI:10.1111/j.1365-2478.1986.tb00513.x.
- Dey A., Morrison H.F., 1979, Resistivity modeling for arbitrarily shaped three-dimensional structures, *Geophysics*, 44, 753-780, DOI:10.1190/1.1440975.
- Dobróka M., Gyulai Á., Ormos Á T., Csókás J., Dresen L., 1991, Joint inversion of seismic and geoelectric data recorded in an underground coal mine, *Geophysical Prospect*, 39, 643-665, DOI: 10.1111/j.1365-2478.1991.tb00334.x.
- Gyulai Á., Dobróka M., Ormos T., Turai E., Sasvári T., 2013, In-mine geoelectric investigations for detecting tectonic disturbances in coal seam structures, *Acta Geophysica*, 61, 1184-1195, DOI:10.2478/s11600-013-0112-6.
- Han D.P., Shi Y.D., 2000a, The numerical simulation of the electrical penetration methods at coal mining working face in roof or floor and in coal seam. *Journal of China Coal Society*, 25, 30~33, DOI: 10.3321/j.issn:0253-9993.2000.z1.007.
- Han D.P., 2000b, Research of the mine electricity penetration method, *Coal Geology & Exploration*, 2000, 28(2): 50-52, DOI: 10.3969/j.issn.1001-1986.2000.02.015.
- Liu Z.X., Xu X.G., Yue J.H., 2003, 3D finite element simulation for mine dc electrical method — research of the dc penetration method, *Computing Techniques for Geophysical & Geochemical Exploration*, 25, 302-307, DOI: 10.3969/j.issn.1001-1749.2003.04.003.
- Lowry T., Allen M.B., Shive P.N., 1989, Singularity removal: a refinement of resistivity modeling techniques, *Geophysics*, 54, 766-774, DOI:10.1190/1.1442704.
- Shi Y.D., 2010, Response characteristics of fault in coal seam sounding curve. *Coal Geology & Exploration*, 38, 55-57, DOI: 10.3969/j.issn.1001-1986.2010.05.012.